

**HORIZON EUROPE PROGRAMME**  
**TOPIC HORIZON-CL4-2022-RESILIENCE-01-24**

**GA No. 101091572**

# **Graphene, MXene and ionic liquid-based sustainable supercapacitor**



## **GREENCAP - Deliverable report**

### **D3.1. – Slurry formulations for high-energy SCs**



**Funded by  
the European Union**

<b>Deliverable No.</b>	GREENCAP D3.1	
<b>Related WP</b>	WP 3	
<b>Deliverable Title</b>	Slurry formulations for high-energy SCs	
<b>Deliverable Date</b>	2025-06-30	
<b>Deliverable Type</b>	REPORT	
<b>Dissemination level</b>	Public (PU)	
<b>Author(s)</b>	Alberto Morengi (BED)	2025-06-13
<b>Checked by</b>	Evie Papadopoulou (BED)	2025-06-24
<b>Reviewed by</b>	Artur Ciesielski (UNISTRA)	2025-06-24
<b>Approved by</b>	Francesco Bonaccorso (BED) - Project coordinator	2025-06-30
<b>Status</b>	Final	2025-06-30

#### Document History

Version	Date	Editing done by	Remarks
V01	2025-06-13	Alberto Morengi	First draft
V02	2025-06-18	Francesco Bonaccorso	Review
V03	2025-06-19	Evie Papadopoulou	Review
V04	2025-06-19	Ahmad Bagheri	Review
V1.0	2025-06-20	Alberto Morengi	
V1.1	2025-06-24	Artur Ciesielski	Reviewer
V2.0	2025-06-30	Francesco Bonaccorso	Final

#### Project summary

GREENCAP project focuses on developing high-performance supercapacitors (SCs) exploiting 2-dimensional materials (2DM) and novel ionic liquid-based (IL) electrolytes leveraging sustainable processes.

Specifically, GREENCAP project addresses all the following aspects of SC production:

- Design of high energy and power density, thermally stable and long life SCs.
- Development of sustainable processes for the electrode production exploiting water-soluble binder, avoiding the use of *N*-methyl-2-pyrrolidone (NMP) and poly-fluoroalkyl substances (PFA)-containing binders.
- Formulation of new electrodes and IL-based electrolytes, avoiding critical raw materials (CRM) and exploiting 2D materials (graphene and MXenes).

- Scale-up of the materials and the establishment of an industrial-chain for SCs production.
- Validation of lab scale SCs (Swagelok cells and pouch cells) and of industrially relevant prototypes (cylindrical cells).

The project goals seek to power the European energy transition providing sustainable and durable energy storage solutions.

## Publishable summary

This deliverable reports the consortium efforts in the design and the formulation of the electrode slurry exploiting two-dimensional (2D) materials, eco-friendly binders and sustainable solvents.

Activated carbon (AC) and curved graphene (CG), proprietary name of the carbide derived carbon (CDC) developed by Skeleton Materials GmbH (SM), are investigated as active materials thanks to their high specific surface area (SSA).

Few-layer graphene (FLG) produced by BeDimensional SpA (BED), electrochemically exfoliated graphene (EG) synthesized by Technische Universität Dresden (TUD), and high-pressure homogenization (HPH) FLG produced by the University of Cambridge (UCAM) are screened as conductive agents. Specifically, their outstanding electrical conductivity enables reduction of the amount of conductive agent and maximize the loading of active material.

A carboxymethyl cellulose (CMC)-based or alginate (Alg)-based compounds are implemented as eco-friendly water-soluble binders substituting the state-of-the-art (SoTA) polyvinylidene fluoride (PVDF). Consequently, water is used as solvent, instead of the teratogenic N-methyl-2-pyrrolidone (NMP), improving the processability and lowering the drying process costs.

Moreover, MXenes, synthesized by Trinity College Dublin (TCD) and Carbon Ukraine (CU), are used for developing electrode slurries and proceeding in their path to the application in supercapacitors.

The Ionogel (IG)-based approach to produce the slurry was investigated aiming at improving the rate capability performances.

The performance and morphology characteristics of the developed slurries are evaluated through a multiplicity of characterization techniques, such as four-probe conductivity measurements, scanning electron microscopy (SEM), cyclic voltammetry (CV) and galvanostatic charge-discharge (GCD) cycling.

## Contents

1	Introduction.....	8
2	Methods and core part of the report.....	10
2.1	Background .....	10
2.2	BeDimensional few-layer graphene-based slurries .....	10
2.3	BeDimensional Ionogel-based slurries.....	13
2.4	Technische Universität Dresden Functionalized electrochemically exfoliated graphene-based slurries .....	14
2.5	Skeleton carbide derived carbon-based slurry .....	14
	Mixing .....	15
2.6	University of Cambridge high-pressure-homogenized few-layer graphene-based slurries	16
2.7	University of Strasbourg functionalized MXene-based slurries.....	17
2.8	BeDimensional MXenes-based slurries.....	17
2.9	Carbon Ukraine free-standing MXene-based slurries.....	18
3	Results & Discussion.....	20
3.1	BeDimensional Few-layer graphene-based slurries .....	20
3.2	BeDimensional Ionogel-based slurries.....	20
3.3	Technische Universität Dresden electrochemically exfoliated graphene-based slurries ....	21
3.4	University of Cambridge Graphene-based slurries.....	23
3.5	Skeleton CDC-based slurry .....	23
	Coating.....	24
3.6	University of Strasbourg functionalized MXenes-based slurries .....	25
3.7	BeDimensional MXene-based slurries .....	25
3.8	Contribution to project (linked) Objectives .....	28
3.9	Contribution to major project exploitable result.....	28
4	Conclusion and Recommendation .....	29
5	Risks and interconnections.....	30
5.1	Risks/problems encountered .....	30
5.2	Interconnections with other deliverables.....	30
6	References.....	31
7	Acknowledgement.....	32

## List of Figures

Figure 1. DFT calculations of pore distribution of a) AC, and b) CG. ....	11
Figure 2. Rs as a function of the composition. a) Conductive agent: comparison between FLG, CB and mixtures. b) Active material: Comparison between CG and AC. The binder used is PVDF.....	12
Figure 3. a) Rs of the slurries based on different binder (X). b,c) flexibility and mechanical resistance of CG:FLG:CMC-LMW (b) and CG:FLG:CMC:SBR (c) slurry-based electrodes. ....	12
Figure 4. Preparation procedure of the IGs-based (right) and conventional electrodes (left). Below it is schematized the electrodes pores wetting with and without the IGs-based method. ....	13
Figure 5. Dissolver processing parameters for the development of graphene-based slurry formulation.....	14
Figure 6. Mixing (left and middle panel) and coating (right panel) of electrode slurries. ....	15
Figure 7. SEM images of a) KS25, b) KS75 and c) KS150 synthetic graphite as the starting material. d), e) and f) shows the corresponding samples after HPH processing into graphene. ....	16
Figure 8. a) Rs and SSA of electrodes made with different HPH graphenes. b) Isotherms of different HPH graphene samples obtained from N <sub>2</sub> adsorption measurements of the electrodes. ....	17
Figure 9. Replacement of traditional MXene deposition method with industrially compatible ones, using flat current collectors instead of foam-type ones. ....	18
Figure 10. a) Mass ratio optimization of the electrode slurry materials. a) Rs as a function of the composition coated on glass slides; b) Comparison of the specific capacitance as a function of the specific current of the electrodes based on CG <sub>90</sub> FLG <sub>5</sub> CMC-SBR <sub>5</sub> and CG <sub>94</sub> FLG <sub>2</sub> CMC-SBR <sub>4</sub> slurry formulation. Electrolyte: 1 M N <sub>1113</sub> FSI in ACN. ....	20
Figure 11. GCD cycles of IG-based a) and conventional b) EDLC at high specific current rates.....	21
Figure 12. Ragone plot of the IG-based EDLC compared to a conventional EDLC based on the same slurry solid content formulation.....	21
Figure 13. Gravimetric capacitance of functionalized graphene (WP2) and graphene (WP1) on carbon fabric b) Cycling performance of functionalized graphene electrodes on carbon fabric c) Gravimetric capacitance of functionalized graphene electrodes in different aqueous electrolytes.....	22
Figure 14. a) Visual comparison of the as-prepared electrodes showing the effect of additives on film quality. b,c) Electrochemical performance of electrodes prepared using slurry formulations with and without additives, respectively. ....	22
Figure 15. a) AFM image of HPH expanded KS25 flake and b) a lateral cross section profile marked out by the white line in a). c) Isotherms of expanded KS25 and HPH expanded KS25 from N <sub>2</sub> adsorption measurements. d) SSA of expanded KS25 and HPH expanded KS25. ....	23
Figure 16. Next generation (GreenCap) coated electrode roll.....	24
Figure 17. a) CV curves of Ti <sub>3</sub> C <sub>2</sub> Tx-BPS in m-xylene and, b) specific capacitance of Ti <sub>3</sub> C <sub>2</sub> Tx (black curve) and Ti <sub>3</sub> C <sub>2</sub> Tx-BPS (red curve) at different scan rates. 1 M H <sub>2</sub> SO <sub>4</sub> was used as aqueous electrolyte, Pt wire as counter electrode and Ag/AgCl as reference electrode. ....	25
Figure 18. Cyclic voltammetry of MXene-based electrodes in the presence of a) 3M H <sub>2</sub> SO <sub>4</sub> , b) 8 m NaNO <sub>3</sub> , and c) 1M KOH in different scan rate ranging from 10 to 500 mV s <sup>-1</sup> . ....	26
Figure 19. Gravimetric capacitances as a function of the specific current measured for MXene-based electrodes produced by slurry method.....	27
Figure 20. Sheet resistance of free-standing MXene-FLG electrodes. ....	28

## List of Tables

Table 1: The slurry recipe. ....	15
Table 2: Typical KPIs of the slurry. ....	24

## Abbreviations & Definitions

Abbreviation	Explanation
<b>2D</b>	Two dimensional
<b>AC</b>	Activated carbon
<b>AFM</b>	Atomic force microscopy
<b>Alg</b>	Alginate
<b>BET</b>	Brunauer-Emmett-Teller
<b>BPS</b>	bis(triisopropoxysilyl)-2,2'-bipyridine
<b>CB</b>	Carbon black
<b>CDC</b>	Carbide derived carbon
<b>CG</b>	Curved graphene
<b>CMC</b>	Carboxymethyl cellulose
<b>CNT</b>	Carbon nanotubes
<b>CRM</b>	Critical raw material
<b>CV</b>	Cyclic voltammetry
<b>DFT</b>	Density functional theory
<b>EDLC</b>	Electrical double layer capacitor
<b>EG</b>	electrochemically exfoliated graphene
<b>EM</b>	Electrode material
<b>ESR</b>	Equivalent Series Resistance
<b>FLG</b>	Few-layer graphene
<b>GCD</b>	Galvanostatic charge-discharge
<b>HMW</b>	High molecular weight
<b>HPH</b>	High pressure homogenized
<b>IG</b>	Ionogel
<b>IL</b>	Ionic liquid
<b>LMW</b>	Low molecular weight
<b>NMP</b>	<i>N</i> -methyl-2-pyrrolidone
<b>PFA</b> s	Poly-fluoroalkyl substances
<b>PVDF</b>	Polyvinylidene fluoride
<b>Rs</b>	Sheet resistance
<b>SC</b>	Supercapacitor
<b>sEG</b>	Functionalized electrochemically exfoliated graphene
<b>SEM</b>	Scanning Electron Microscope
<b>SoTA</b>	State-of-the-art
<b>SSA</b>	Specific surface area

# 1 Introduction

This deliverable presents the development of electrode slurry formulations aimed at meeting the performance targets for high-energy supercapacitors (SCs), with a particular focus on sustainability and simplification of the production process. The optimized slurry composition integrates curved graphene (CG) as the active material, few-layer graphene (FLG) as the conductive additive, and a water-soluble carboxymethyl cellulose-styrene butadiene rubber (CMC-SBR) as the binder.

It should be mentioned that FLG enhances the electrical conductivity of the electrode, allowing for a reduction in the amount of conductive additive required, while increasing the content of the active material (e.g., CG), thereby improving the energy storage properties of the electrodes.

The selected binder combination, in contrast to the conventional polyvinylidene fluoride (PVDF), is both fluorine-free and water-compatible. This eliminates the need for N-Methyl-2-pyrrolidone (NMP), a toxic and high-boiling solvent, thereby reducing environmental impact and energy consumption during processing.

This work has been conducted within the framework of WP3, which aims to develop and optimize sustainable electrode formulations and processes, and to fabricate and validate lab-scale pouch cells. The outcomes of WP3 will serve as a basis for WP4, which focuses on the industrial upscaling of electrodes and the development of cylindrical cell prototypes.

WP3 is divided into three main tasks:

- Task 3.1: Electrode slurry formulation  
It consists in the development of the electrode slurry, which is the core content of this deliverable.
- Task 3.2: Electrode fabrication and characterization  
It consists in the fabrication and in the scaling up of the electrodes with the formulated slurry, optimizing the processes, the electrode thickness, the mechanical and electrochemical properties.
- Task 3.3: Lab-scale SC development and optimization  
Pouch cells prototyping and evaluation of their overall performances.

Key achievements:

- Sheet resistance lower than  $100 \Omega/\square$ , reaching  $24 \pm 1 \Omega/\square$  in case of CG:FLG:PVDF (80:10:10).
- Maximization of the active material content (CG), up to 94 w%, and, therefore, of the gravimetric capacity and of the specific energy, whilst maintaining a sheet resistance lower than  $100 \Omega/\square$ .
- Implementation of sustainable fluorine-free water-based binder (CMC-based), minimizing the footprint of the electrodes and of their production processes.



- Implementation of IG-based slurry. It simplifies the cell production process, eliminating the pre-filling step and improves the rate performances, thanks to the higher electrolyte permeation in the electrodes.
- Easy processability through printing deposition techniques, such as doctor blading.

Deviation:

- In terms of surface area, although CG has a SSA lower than 2000 m<sup>2</sup>/g (1374 m<sup>2</sup>/g), its graphitic structure is advantageous to improve the capacitance normalised to the SSA compared to that of a conventional activated carbon (AC) with a higher SSA of 1694 m<sup>2</sup>/g. It is also worth mentioning that in the project we can produce carbonaceous materials with surface areas greater than 2000 m<sup>2</sup>/g, but their defective structures negatively affect their electrical conductivity and capacitance.

## 2 Methods and core part of the report

### 2.1 Background

State-of-the-art (SoTA) electrode slurries typically utilize carbon-based materials with high SSA as active components. ACs, in particular, offer excellent ionic accessibility and can achieve high specific capacitance in organic electrolytes. However, their inherently low electrical conductivity necessitates the use of conductive additives including carbon black (CB), which provides negligible capacitance on its own. Due to the limited conductivity of CB, especially when compared to graphene-related materials, the proportion of active material in the electrode is often restricted to below 90 wt%, which adversely impacts the specific capacitance and overall energy storage capability.

PVDF is widely used as the SoTA binder because of its excellent mechanical and thermal stability and its solubility in organic solvents including NMP, enabling the preparation of stable and homogeneous slurries. However, the PVDF/NMP system poses several challenges related to safety, environmental impact, and process efficiency. Furthermore, NMP is a teratogenic solvent that requires dedicated industrial infrastructure and stringent personal protective measures for safe handling, recycling, and disposal. Moreover, its removal from the electrode requires energy-intensive drying. PVDF, being a fluorinated polymer containing per- and polyfluoroalkyl substances (PFAs), raises serious environmental concerns due to its persistence and toxicity.

The GREENCAP project aims to overcome these limitations by formulating sustainable, high-performance electrode slurries using graphene-based materials and water-soluble, PFA-free binders.

### 2.2 BeDimensional few-layer graphene-based slurries

At BED, electrode slurries were prepared by mixing active materials, either CG or AC, with conductive additives (FLG or CB) in powder form, followed by the incorporation of binder solutions based on either PVDF or CMC. Milli-Q water and NMP were used as solvents for the CMC- and PVDF-based binders, respectively. The final solid-to-liquid weight ratio of the slurry was 33:67.

At the laboratory scale, the carbonaceous powders were initially mixed with half of the total solvent mass (approx. 33.3% of the slurry mass) using a Thinky® planetary mixer. Meanwhile, the binder was dissolved in the remaining solvent portion. This binder solution was then combined with the powder dispersion, and the mixture underwent a second round of planetary mixing (10 minutes at 2000 rpm), followed by a 40-second defoaming step at 2200 rpm. For PVDF-based systems, the binder solution was pre-heated to 60 °C to ensure full dissolution and homogeneity.

To ensure uniform particle dispersion and optimize mixing conditions, slurry quality was assessed using a grindometer. Multiple mass ratios of active material, conductive additive, and binder were investigated with the objective of minimizing inactive components while maximizing the load of electrochemically active material, thereby improving the specific capacitance.

The electrical performance of the slurries was evaluated by measuring sheet resistance ( $R_s$ ) using a four-probe conductivity setup. Film thickness, required for conversion from  $R_s$  to bulk conductivity, was determined using a micrometer with 1  $\mu\text{m}$  resolution. To assess both intrinsic material

conductivity and practical electrode performance, the slurries were deposited on glass substrates and aluminum foils coated with carbon.

### Active material, conductive agent and binder selection

At BED, the selection of active materials focused on two candidates: CG, a proprietary carbide-derived carbon (CDC) developed by Skeleton Materials (SM), and a commercial activated carbon (AB520Y) purchased from MTI Corporation.

The specific surface area of these materials was characterized through N<sub>2</sub> and CO<sub>2</sub> physisorption at 77 K and 273 K, respectively. The Brunauer–Emmett–Teller (BET) method was employed to assess mesoporous and macroporous regions (pores >1 nm) via N<sub>2</sub> physisorption, while the microporous structure was investigated using CO<sub>2</sub> physisorption analyzed by density functional theory (DFT). CG and AC exhibited BET SSAs of 1374 m<sup>2</sup>/g and 1694 m<sup>2</sup>/g, respectively.

Interestingly, although the BET surface area of AC is higher, DFT analysis revealed that CG possesses a more pronounced microporous structure. This is reflected in the cumulative micropore surface area and pore size distribution reported in Figure 1, which highlights the superior microporosity of CG relative to AC.

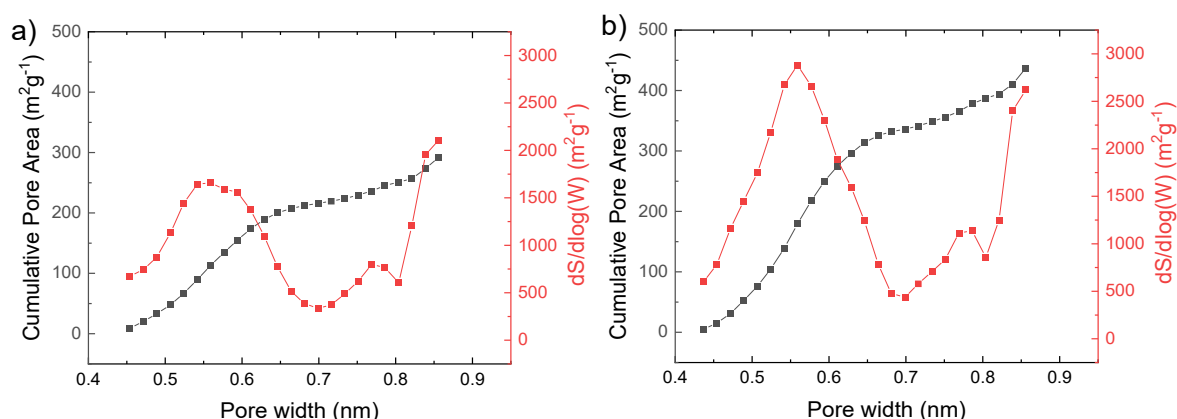


Figure 1. DFT calculations of pore distribution of a) AC, and b) CG.

For the evaluation of active materials and conductive agents, the  $R_s$  of the electrode formulations was measured without the influence of the current collector, i.e., by depositing the slurries onto glass slides. The reference slurry followed the SoTA formulation, consisting of active material, conductive agent, and PVDF in a mass ratio of 80:10:10. Commercial AC (AB520Y) and CB were used as benchmarks for the active and conductive phases, respectively.

Furthermore,  $R_s$  was calculated from the measured conductivity, assuming an electrode thickness of 80  $\mu\text{m}$  as a representative value. The results are presented in Figure 2. Specifically, Figure 2a compares different mass ratios of CB and FLG, while keeping the amounts of CG and PVDF constant. In contrast, Figure 2b explores variations in the mass of FLG and the active material, with the PVDF content held fixed.

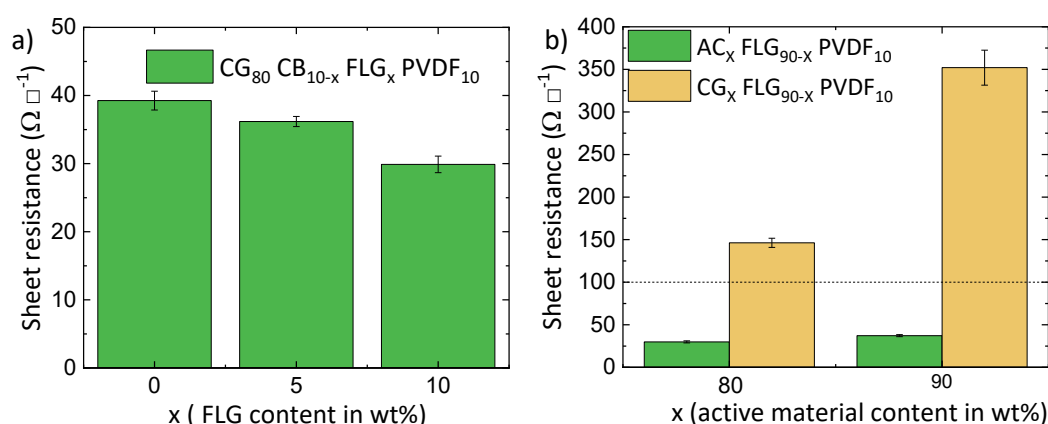


Figure 2.  $R_s$  as a function of the composition. a) Conductive agent: comparison between FLG, CB and mixtures. b) Active material: Comparison between CG and AC. The binder used is PVDF.

The conductivity of the electrodes increased with the substitution of the AC and CB with CG and FLG, respectively. Specifically, the use of CG without the conductive agent resulted in the decrease of the  $R_s$  to  $37 \Omega/\square$ , which is lower than the  $R_s$  of AC in the absence of a conductive agent ( $352 \Omega/\square$ ) (Figure 2b). Furthermore, FLG exhibited higher conductivity than CB resulting in a decrease of the  $R_s$  of the electrode from  $39 \Omega/\square$  to  $30 \Omega/\square$ .

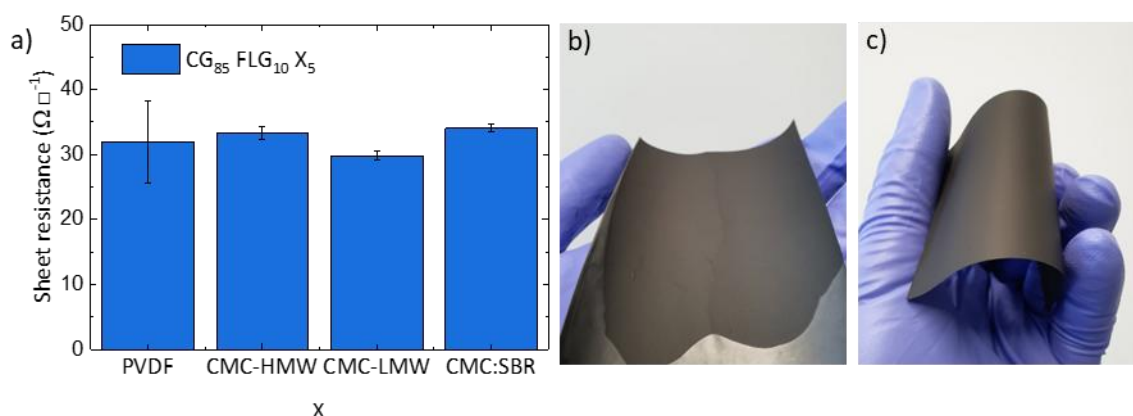


Figure 3. a)  $R_s$  of the slurries based on different binder (X). b,c) flexibility and mechanical resistance of CG:FLG:CMC-LMW in (b) and CG:FLG:CMC:SBR in (c) slurry-based electrodes.

To address concerns related to the use of PFAs-containing binders and the toxic solvent NMP, an eco-friendly, water-soluble CMC-based binder was investigated. Specifically, both low and high molecular weight (HMW) variants (CMC-low molecular weight (LMW) and CMC-HMW, respectively) were evaluated. To enhance the mechanical stability and uniformity of the electrodes, critical for scale-up and processing under mechanical stress conditions such as roll-to-roll fabrication, styrene-butadiene rubber (SBR) was added alongside CMC. The combination improves the electrode resistance to deformation, cracking, and surface defects during handling and manufacturing.

All slurries formulated with CG and FLG at fixed mass ratios (Figure 3a) demonstrated similar  $R_s$  values ( $30\text{--}35 \Omega/\square$ ), confirming the effective replacement of the SoTA PVDF binder with the more sustainable CMC-based alternative. These results also indicate excellent compatibility of CMC with both CG and FLG. Moreover, the addition of SBR significantly improved the mechanical robustness and flexibility of the electrode films, ensuring strong adhesion and surface durability without compromising electrical conductivity (Figures 3b and 3c).

## 2.3 BeDimensional Ionogel-based slurries

At BED, the production of IG-based slurries was carried out following a method adapted from the process developed and patented by SOLV (Patent no. WO2020260444 A1). Specifically, AC, which is used as the active material, was mixed with FLG (conductive agent), CMC-SBR (binder) with the 1-ethyl-3-methylimidazolium bis(fluorosulfonyl)imide (EMISFI) IL, using water as solvent. The solid content weight ratio % was 90:5:5, the IL:water ratio was 1:1 and the solid:liquid content ratio was 1:3 wt/wt. The mixture was prepared using a planetary centrifugal mixer. Once a homogeneous slurry was obtained, it was cast on carbon coated aluminium collectors by doctor blading and dried at 70°C in dynamic vacuum overnight. The described procedure is schematized in Figure 4. The conventional and IG approaches wetting behaviours are compared in the lower panels of Figure 4, depicting the main difference: The IG approach, in contrast to the conventional one, ensures a complete wetting of the electrode surface reaching even the smaller pores without suffering from pore gas trapping, which usually limits the wettability of the micropores in conventional electrodes.

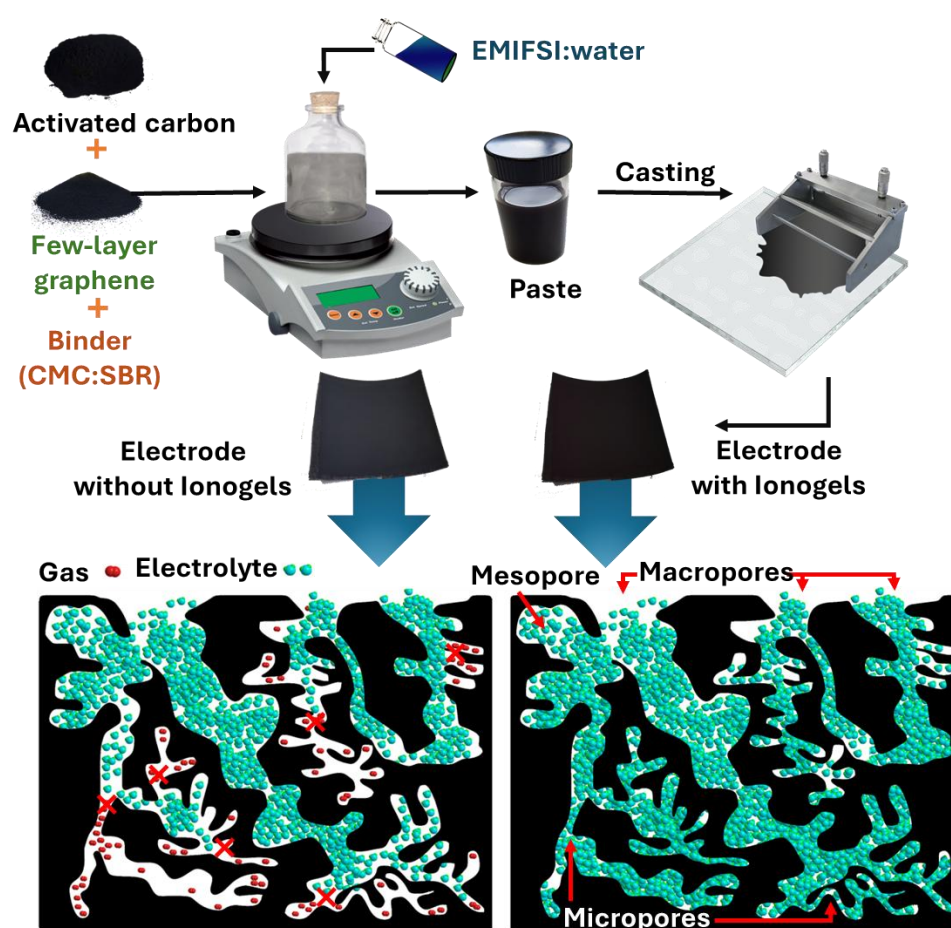


Figure 4. Preparation procedure of the IGs-based (right) and conventional electrodes (left). Below it is schematized the electrodes pores wetting with and without the IGs-based method.

## 2.4 Technische Universität Dresden Functionalized electrochemically exfoliated graphene-based slurries

At TUD, the focus is on developing sustainable and environmentally friendly slurry formulations that are compatible with scalable coating techniques and adaptable to a variety of current collectors. Conventional active materials including AC exhibit low electrical conductivity and limited processability, necessitating the inclusion of conductive additives and polymeric binders to achieve satisfactory electrochemical and mechanical performance.

To address these limitations, TUD has developed polyaniline-functionalized graphene (sEG) through electrochemical exfoliation, as part of **WP1** and **WP2**. This material demonstrates both high electrical conductivity and excellent processability, enabling its direct use as an electrode material (EM). As a result, the amount of conductive additive required can be significantly reduced, or even eliminated, leading to improved capacitance and overall device performance.

However, the degree of adhesion between the EM and the current collector may vary depending on the surface characteristics of the substrate. In such cases, the inclusion of a minimal amount of binder may still be necessary to ensure adequate mechanical stability and contact integrity.

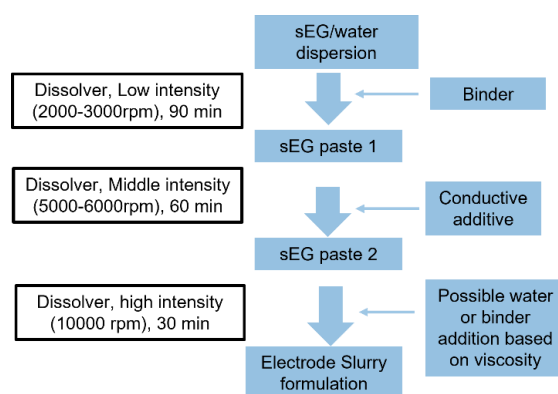


Figure 5. Dissolver processing parameters for the development of graphene-based slurry formulation.

To produce a graphene-based slurry formulation, we optimized the dissolver process as follows:

1. Binder, sEG and water were mixed and processed using a dissolver at a speed of 2000–3000 rpm for 90 minutes.
2. The conductive additive (CB) was then added to the mixture, followed by further dispersion using the dissolver at medium intensity (5000–6000 rpm) for 60 minutes.
3. Finally, the viscosity of the mixture was adjusted by either adding water to reduce viscosity or binder to increase it, using high-intensity mixing (6000–10000 rpm) for 30 minutes.

The details of the developed process are shown in Figure 5.

## 2.5 Skeleton carbide derived carbon-based slurry

### Particle size

A grindometer is used to determine the particle size in the slurry. Particles must not be below a threshold size of 10  $\mu\text{m}$ .

### Solid content



The solid content is determined using a Sartorius infrared moisture analyser. The target value is 33%.

#### Viscosity

Viscosity is determined using a Brookfield viscosimeter and it is expected to be below 1050 cP.

#### Temperature

The temperature of the slurry must be monitored before the addition of acrylic binder and should not exceed 40 °C.

### Mixing

The mixing procedures for AC and CG are very similar, however fine tuning of various parameters is required respectively for each.



Figure 6. Mixing (left and middle panel) and coating (right panel) of electrode slurries.

Using an industrial mixer, half of the EM and the entire quantity of CB as the conductive additive were added to the mixing bowl in the proportions specified in Table 1. Sodium carboxymethylcellulose (Na-CMC), an industry-standard dispersive binder, was manually weighed and added to the dry mixture. The powders were then mixed for approximately one minute to ensure homogeneous blending. Subsequently, the remaining portion of the EM was combined with water and added to the mixture, bringing it to the kneading point. After kneading, the mixture was further diluted. An acrylic binder was then incorporated, and the slurry was gradually diluted and sampled until the required process and material specifications were achieved.

The final slurry was transferred to a shipping container, and representative samples were collected from the residual material remaining in the equipment for quality control and characterization purposes.

Table 1: The slurry recipe.

	Typical AC SCs (% dry mass)	Greencap prototype (% dry mass)
Na-CMC	< 2.0	< 2.0
YP 50/ CDC	Up to 93.0	Up to 95.0
CB	< 3.0	< 1.0
Acrylic binder	< 3.0	< 3.0

## 2.6 University of Cambridge high-pressure-homogenized few-layer graphene-based slurries

UCAM investigated and optimised the use of HPH for the large-scale liquid exfoliation of graphene for SC EM. Slurries using graphene material as developed in WP2 will be formulated and made into SC electrodes using blade coating. Their  $R_s$  and SSA will be characterised.

As the flake size of the HPH graphene strongly influences their overall electrical conductivity and surface area, UCAM first prepared electrodes using graphene made from synthetic graphite with different initial flake sizes, KS25, KS75 and KS150. The number in the sample name refers to the average flake size. Figure 7 shows the SEM images of the different synthetic graphite samples before and after HPH processing into graphene. The final average flake size of the HPH graphene made from KS25, KS75 and KS150 were found to be 1.2  $\mu\text{m}$ , 2.8  $\mu\text{m}$  and 6.1  $\mu\text{m}$  respectively.

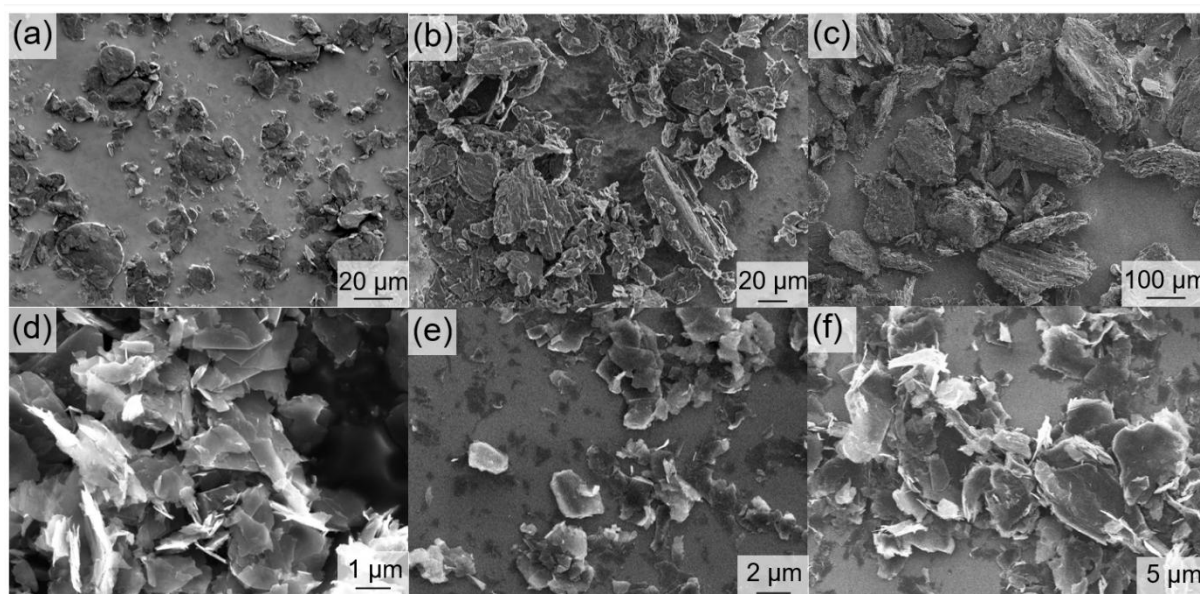


*Figure 7. SEM images of a) KS25, b) KS75 and c) KS150 synthetic graphite as the starting material. d), e) and f) shows the corresponding samples after HPH processing into graphene.*

An aqueous slurry consisting of 4 wt.% CMC and SBR with respect to the HPH graphene was made and used to fabricate SC electrodes. The  $R_s$  and SSAs of the electrodes were measured using a 4 point-probe and  $\text{N}_2$  gas adsorption measurements, respectively (Figure 8). Owing to the high conductivity of graphene, the  $R_s$  of all electrodes was  $\leq 2.7 \Omega/\square$ , which is well below the KPI goal of  $< 100 \Omega/\square$ . The  $R_s$  decreased with increasing flake size since the in-plane electrical conductivity of graphene is much higher than the inter-flake conductivity and eliminate the contact resistances. The SSA of the electrodes also decreased with increasing flake size. This could be due to larger flakes being more difficult to exfoliate, or simply due to larger flakes intrinsically having lower surface area to volume ratios. The measured isotherms show a hysteresis over a large pressure range upon gas desorption, which is a typical H3 hysteresis. This is as expected as this type of hysteresis generally indicates the presence of slit-shaped pores which is consistent with the structure of graphene-based electrodes. Given that a high specific area is desirable in EMs, coupled with the low  $R_s$  achieved in all 3 samples, UCAM will proceed with using KS25 as the starting material for further optimisation.



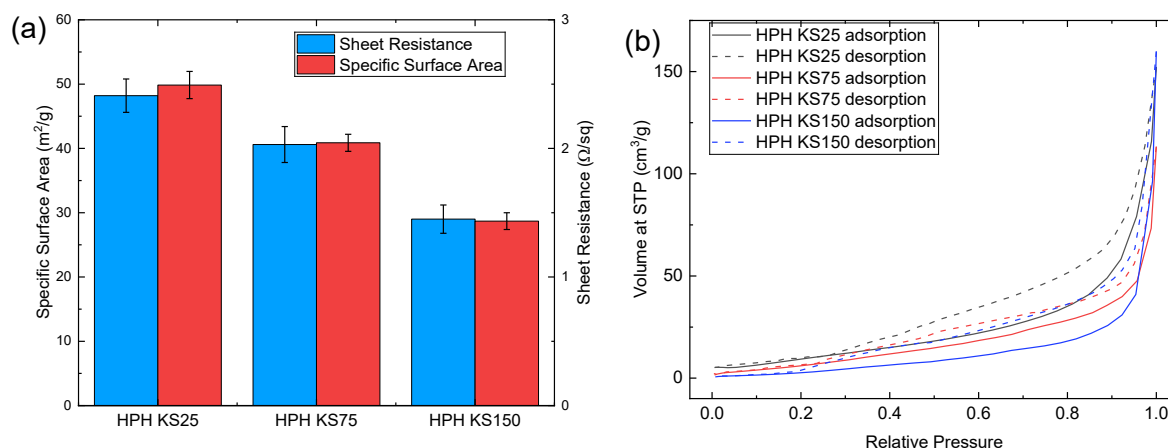


Figure 8. a)  $R_s$  and SSA of electrodes made with different HPH graphenes. b) Isotherms of different HPH graphene samples obtained from  $N_2$  adsorption measurements of the electrodes.

## 2.7 University of Strasbourg functionalized MXene-based slurries

UNISTRA has developed water-based electrode slurry formulations for the  $Ti_3C_2T_x$  MXene powder provided by TCD, including both pristine and functionalized materials. The functionalization with 5,5'-bis(triisopropoxysilyl)-2,2'-bipyridine (BPS) was performed at UNISTRA in three different solvents, ethanol, isopropanol, and *m*-xylene, to evaluate the impact of processing medium on electrode properties. Both  $Ti_3C_2T_x$  and  $Ti_3C_2T_x$ -BPS materials were dispersed in ethanol and directly drop-cast onto circular carbon paper electrodes (1.2 cm diameter), followed by vacuum drying at 80 °C overnight. The resulting electrodes, with a mass loading of approximately 1 mg/cm<sup>2</sup>, were mechanically robust, binder-free, and compatible with simple scalable deposition methods, aligning with the formulation goals of Task 3.1.

Electrical conductivity measurements of the dried films have shown that pristine  $Ti_3C_2T_x$  exhibited a high value of 4767 S/cm. Upon functionalization, the conductivity decreased depending on the solvent used. The sample prepared in *m*-xylene retained a relatively high conductivity of 1956 S/cm, while those processed in ethanol and isopropanol showed lower values of 892 and 1180 S/cm, respectively. This reduction is attributed to the incorporation of organic groups, though the *m*-xylene sample maintained sufficient conductivity for effective charge transport.

## 2.8 BeDimensional MXenes-based slurries

MXenes, a class of two-dimensional (2D) transition metal carbides and nitrides, have gained significant attention for electrochemical energy storage due to their metallic conductivity, high SSA, and tunable interlayer spacing. Their unique structure allows for efficient ion intercalation and surface redox reactions, making them strong candidates for use as SC electrodes. However, the conventional fabrication method — typically vacuum filtration — limits scalability and compatibility with industrial processes (Figure 9).

In this activity, BED focused on the electrochemical characterization of MXene materials synthesized and provided by TCD. The main objective was to assess the performance of these MXenes as active

EMs for SC applications, using a scalable and industry-compatible slurry-based deposition method. The study also aimed to compare the performance of MXene electrodes in various aqueous electrolytes (acidic, neutral, and basic) to understand the effect of electrolyte environment on their capacitive behavior.

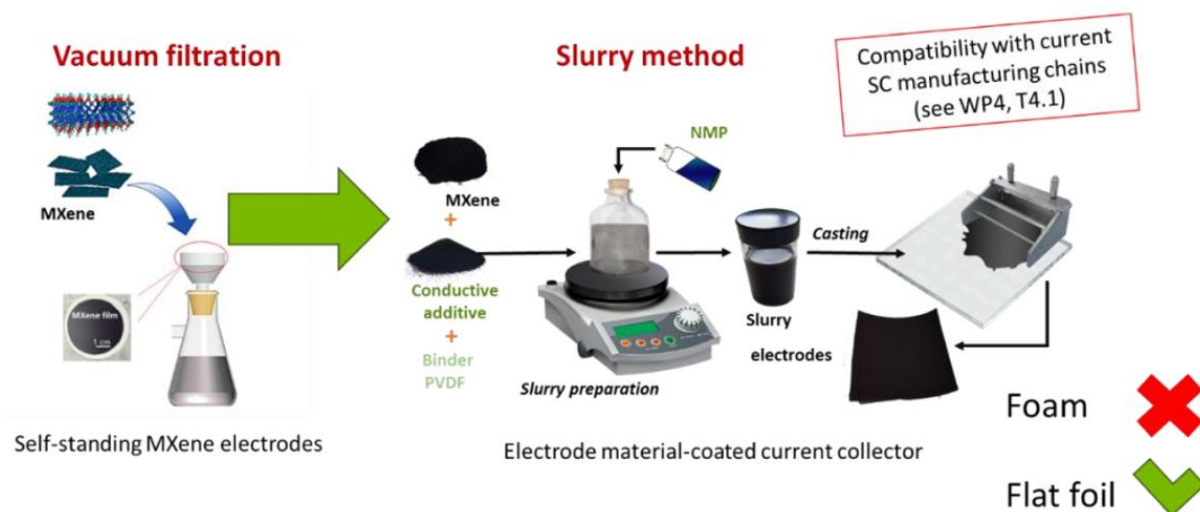


*Figure 9. Replacement of traditional MXene deposition method with industrially compatible ones, using flat current collectors instead of foam-type ones.*

The electrode formulation was based on a ternary mixture of MXene, FLG, and PVDF in a 90:5:5 weight ratio. The MXene powder, synthesized by TCD, was dispersed in NMP, which acted as the solvent. Subsequently, FLG was added as both a conductive additive and a mechanical spacer. Its role was to enhance electrical conductivity, improve electrolyte accessibility, and simultaneously prevent the restacking of MXene layers. PVDF was used as the binder and was pre-dissolved in NMP before being incorporated into the mixture. The slurry was homogenized in a sonic bath for one hour to ensure proper mixing and dispersion. It was then cast onto flat graphite paper substrates using the doctor blade method, an industrially compatible approach that allows for uniform and controllable film thickness. The cast films were dried overnight at 60 °C, followed by vacuum drying at 120 °C for 12 h to remove residual solvent. Final electrode mass loading was maintained between 1 and 2 mg cm<sup>-2</sup>. Electrochemical measurements were performed in a Swagelok three-electrode setup using either Ag/AgCl or Hg/HgO reference electrodes and a high-mass-loading AC counter electrode. The electrodes were tested in three aqueous electrolytes, including acidic (3 M H<sub>2</sub>SO<sub>4</sub>), neutral (8 m NaNO<sub>3</sub>) and alkaline (1 M KOH) conditions. Cyclic voltammetry (CV) scans were carried out at scan rates ranging from 10 to 500 mV s<sup>-1</sup>. Galvanostatic charge–discharge (GCD) tests were conducted across a wide current density range from 0.1 to 20 A g<sup>-1</sup>.

## 2.9 Carbon Ukraine free-standing MXene-based slurries

A second approach used for the production of MXenes electrodes is the vacuum filtration and results in free-standing films of MXenes. Specifically, following the recipe provided by TCD, the solution of MXenes and dionized water, eventually mixed with carbonaceous powders, is vacuum-filtered through a porous membrane (e.g., Celgard or polypropylene) to form a uniform, flexible, and mechanically stable free-standing film. These films are then dried under vacuum at room temperature or slightly elevated temperature (e.g., 60 °C) and can be directly used as working electrodes without the need for

binders or conductive additives. This fabrication approach ensures high conductivity, excellent ion accessibility and structural integrity, suitable for electrochemical characterization in a three-electrode cell configuration.

Within WP2, CU synthesized a variety of MXene materials with tailored surface properties and distributed them to several project partners for collaborative testing, characterization, and slurry formulation development. These materials were provided in different formats, including pre-dispersed pristine MXene slurries and ready-made composite electrodes with customized compositions, depending on the specific needs and research focus of each partner.

To support diverse experimental strategies, CU employed multiple approaches for the preparation of electrode compositions, including:

- Mixing multilayer and single-layer MXenes in various ratios;
- Combining MXenes with commercial activated carbon (YP50F);
- Blending MXenes with nanoporous CDC, both synthesized in-house by CU;
- Integrating MXene materials with graphene supplied by BeDimensional.

These tailored materials enabled cross-validation and co-development of slurry formulations and electrode structures across different laboratories. The following partners received CU's MXene-based samples for specific collaborative activities:

- **UNISTRA** – for electrochemical testing;
- **FSU** – for electrochemical testing;
- **BeDimensional** – for electrochemical testing;
- **University of Cambridge** – for optical and surface characterization;
- **TUD** – for slurry formulation development.

### 3 Results & Discussion

#### 3.1 BeDimensional Few-layer graphene-based slurries

At BED, the mass ratio optimization (Figure 10a) is carried out focusing on the maximization of the active material (CG) without compromising the  $R_s$  value (kept below  $100 \Omega/\square$ ) and therefore the rate performance of the electrode slurry. Specifically, FLG amount is decreased to 2 wt.% while the binder quantity is lowered to 4 wt.% in order not to compromise the mechanical properties and the industrial processability of the slurry. Consequently, the  $R_s$  increased to  $66 \Omega/\square$ , which is still acceptable being lower than  $100 \Omega/\square$ . The reduction of FLG (from 5% to 2%) and that of the binder (from 5% to 4%) enabled an increase in the electrode gravimetric capacitance at 0.2 A/g of the 94:2:4 composition by ca. 5 % (Figure 10b) with respect the 90:5:5 composition.

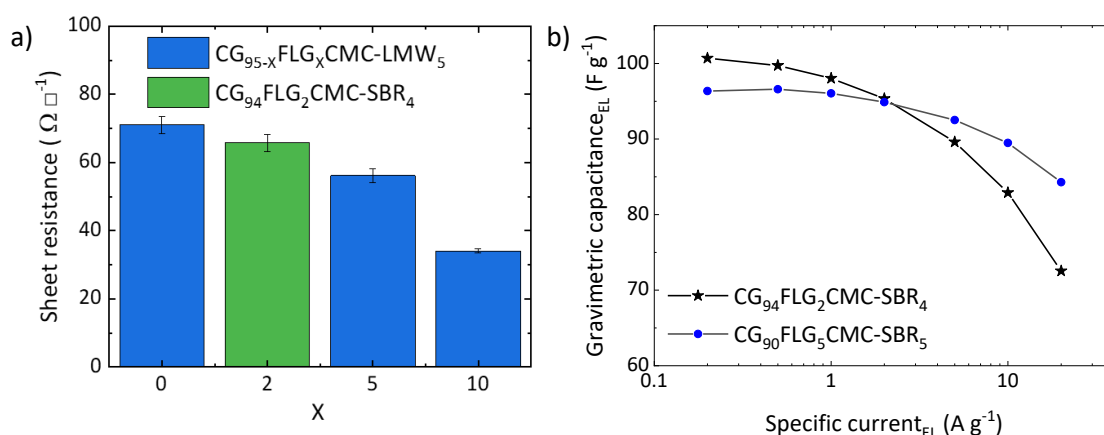


Figure 10. Mass ratio optimization of the electrode slurry materials. a)  $R_s$  as a function of the composition coated on glass slides; b) Comparison of the specific capacitance as a function of the specific current of the electrodes based on  $CG_{90}FLG_5CMC-SBR_5$  and  $CG_{94}FLG_2CMC-SBR_4$  slurry formulation. Electrolyte: 1 M  $N_{1113}FSI$  in ACN.

Finally, the CG:FLG:CMC-SBR (94:2:4) slurry has been deposited by doctor blading on carbon coated aluminium collectors. The electrode obtained with a thickness of  $70 \mu m$  and a mass loading of  $5.2 mg/cm^2$  exhibited a  $R_s$  of  $220 m\Omega/\square$  and a conductivity of  $5.6 \times 10^4 S/cm$ . The low  $R_s$  value demonstrates an optimum electrical connection between the EMs and the current collector.

#### 3.2 BeDimensional Ionogel-based slurries

At BED, the IG-based slurries were used for building symmetric electrical double layer capacitors (EDLC) and tested with GCD cycles to assess the improved rate performances with respect to the conventional electrode fabrication approach.

The GCD cycles of IG-based EDLC (Figure 11a) exhibit a more triangular shape than the GCD of the conventional EDLC (Figure 11b) and a lower equivalent series resistance (ESR), which is reduced from  $1.85 \Omega$  (conventional EDLC) to  $1.2 \Omega$  (IG-EDLC), evaluated for an electrode with indicative diameter of 15 mm and with a mass loading of  $4 mg cm^{-2}$ .

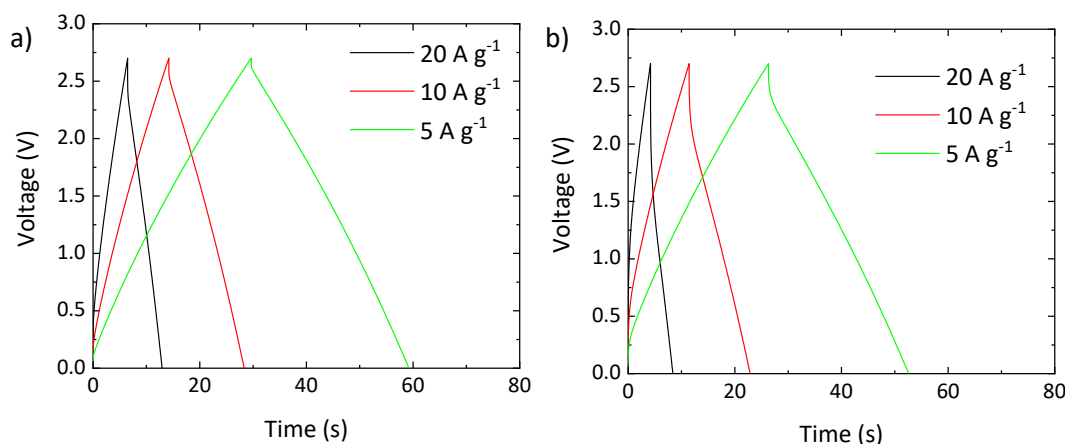


Figure 11. GCD cycles of IG-based a) and conventional b) EDLC at high specific current rates.

The low ESR achieved using the IGs approach enabled to improve the rate capability performance of the EDLC. In fact, as shown in Figure 12, while the energy density at  $140 \text{ W kg}^{-1}$  are similar ( $30 \text{ Wh kg}^{-1}$  for the IGs-EDLC vs  $29 \text{ Wh kg}^{-1}$  for the conventional one), when the power density increase exceeding  $10 \text{ kW kg}^{-1}$ , the IG-based EDLC retains more than the 80 % ( $25 \text{ Wh kg}^{-1}$  at  $13 \text{ kW kg}^{-1}$ ) of its initial energy density. On the contrary, the energy density of conventional EDLC drops by 66 % ( $10 \text{ Wh kg}^{-1}$  at  $10 \text{ kW kg}^{-1}$ ).

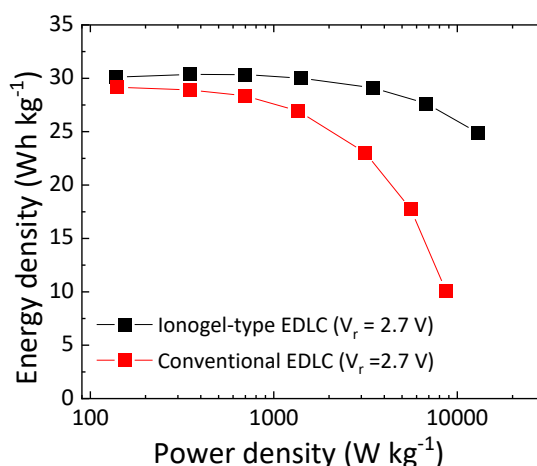


Figure 12. Ragone plot of the IG-based EDLC compared to a conventional EDLC based on the same slurry solid content formulation.

### 3.3 Technische Universität Dresden electrochemically exfoliated graphene-based slurries

At TUD, we initially developed water-based inks and pastes for functionalized graphene **without binders and conductive additives** and produced them on various current collectors such as carbon fabric, titanium and aluminum.

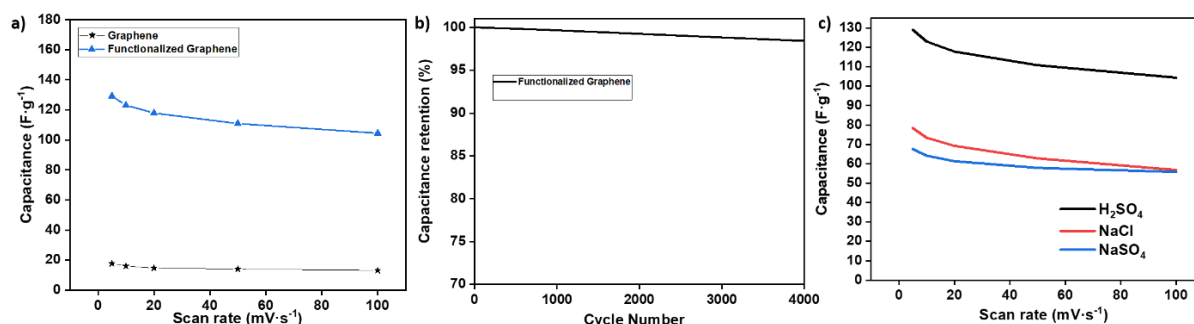


Figure 13. Gravimetric capacitance of functionalized graphene (WP2) and graphene (WP1) on carbon fabric b) Cycling performance of functionalized graphene electrodes on carbon fabric c) Gravimetric capacitance of functionalized graphene electrodes in different aqueous electrolytes.

In this context, the functionalized graphene ink/paste formulation was successfully fabricated on a carbon fabric current collector without binders and conductive additives. The developed electrodes exhibit good performance, including high specific capacitance, high speed and high cycling stability. We also investigated the electrolyte effect with acidic and neutral water-based electrolytes, including  $\text{H}_2\text{SO}_4$ ,  $\text{NaCl}$  and  $\text{NaSO}_4$  (Figure 13). The results show that neutral electrolytes decrease the capacitance due to the low activation of the redox functional group on graphene. However, functionalized graphene in  $\text{NaCl}$  shows a twofold increase in capacitance over graphene. It is important to mention that the use of neutral electrolytes is safer for portable applications and prevents corrosion inside the SC (e.g. corrosion of metallic current collectors). Unfortunately, the fabricated functionalized graphene was not stable on other current collectors such as titanium and aluminum which caused the fabricated layer to detach from the surface (Figure 14a). Therefore, we started to develop slurry formulations by adding minimal amounts of binders and conductive additives. We used different water-soluble binders (e.g., CMC, alginate (Alg), polyvinyl alcohol) and conductive additives (e.g. CB, carbon nanotubes (CNT)) in different ratios and tested their fabrication on titanium and aluminium substrate (Figure 14a). The best formulation was obtained with (functionalized graphene: CB: Alg, 8:1:1) in terms of the film mechanical stability, conductivity (Alg shows **1.5-2 times** better film electrical conductivity than CMC) and achieved a higher performance compared to the formulation without additives (Figure 14b and c).

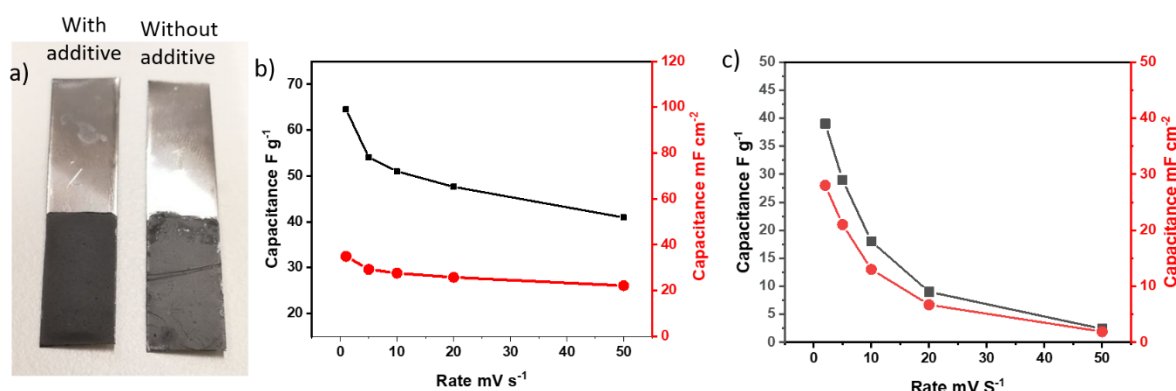


Figure 14. a) Visual comparison of the as-prepared electrodes showing the effect of additives on film quality. b,c) Electrochemical performance of electrodes prepared using slurry formulations with and without additives, respectively.

### 3.4 University of Cambridge Graphene-based slurries

To further increase the SSA of the HPH graphene, **UCAM** used microwave expansion of KS25 prior to HPH exfoliation to improve the exfoliation efficiency of the HPH graphene. This was done by first intercalating KS25 with perchloric acid, followed by subjecting the samples to microwave heating. Figures 15a and b show an atomic force microscopy (AFM) image and cross section profile of a typical HPH expanded KS25 flake. The lateral size of the flake is much larger compared to flakes made by HPH on KS25 without expansion. N<sub>2</sub> adsorption measurements were performed on the expanded KS25 before and after HPH for comparison (Figure 15c). The SSA of the expanded KS25 is 156 m<sup>2</sup>/g, higher than the starting KS25 graphite, and higher than HPH KS25. The SSA was further increased to 600 m<sup>2</sup>/g after processing the expanded KS25 using HPH (Figure 15d). The Rs of electrodes made using the HPH expanded KS25 was ~2 Ω/sq, more conductive than electrodes made using HPH KS25.

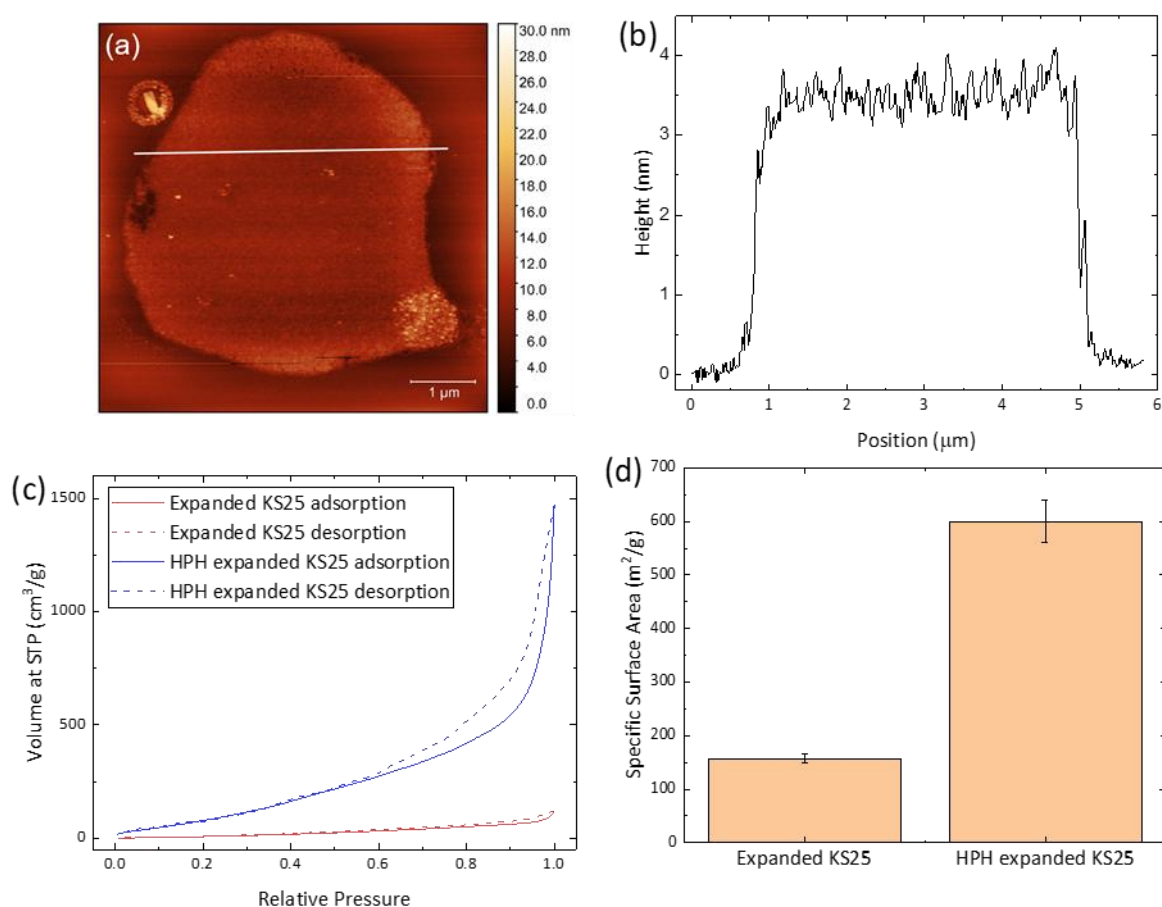


Figure 15. a) AFM image of HPH expanded KS25 flake and b) a lateral cross section profile marked out by the white line in a). c) Isotherms of expanded KS25 and HPH expanded KS25 from N<sub>2</sub> adsorption measurements. d) SSA of expanded KS25 and HPH expanded KS25.

### 3.5 Skeleton CDC-based slurry

The trials searching for optimized mixing parameters for CG were successful. The YP-50 information was taken as a basis, which was produced with the required viscosity and grind with a total content of solids of 1/3. Similarly, the CG slurry was produced within the specified viscosity and grind. Trials have shown that higher solid contents facilitate the subsequent drying step after coating which leads to increased compaction density. This results in a higher density material coated on the final product



(Figure 16), which then increases the overall capacitance of the SC cell. Therefore, the solid content with CG was raised. The typical KPIs of the slurries are listed in Table 2.

*Table 2: Typical KPIs of the slurry.*

Mix No.	Volume (L)	Total Slurry (kg) / Binder (kg)	Final Solid Content (%S)	Final Viscosity (mPa.s) at 100 1/s	Grindo (μm)	Density (g/cm <sup>3</sup> )
<b>Activated Carbon</b>						
1	5	< 3.2	< 35%	<1050	15	1.2
2	5	< 3.2	< 35%	<850	8	1.2
3	50	< 3.2	< 35%	<850	8	1.2
4	50	< 3.2		<850	8	1.2
<b>Curved Graphene</b>						
1	5	< 3.0	< 45%	<850	8	1.2
2	50	< 3.0	< 45%	<1050	10	1.2
3	50	< 3.0	< 45%	<1050	10	1.2

## Coating

The coating was performed in two phases.

1. Phase one - standard AC slurry was used for setting base parameters.
  - a. Standard parameters for the machines were used at a coating speed of 10 m/min.
2. Phase two consisted of coating aluminum-foil current collector using the CG slurry (Figure 16). Due to the reduced weight of the coat needed, drying times had to be optimized.



*Figure 16. Next generation (GreenCap) coated electrode roll.*



### 3.6 University of Strasbourg functionalized MXenes-based slurries

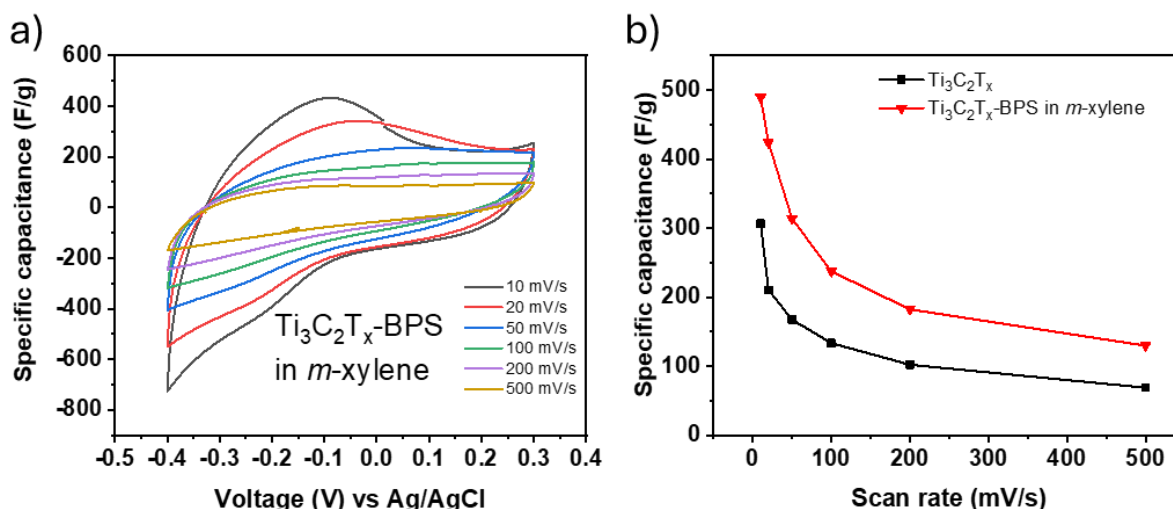


Figure 17. a) CV curves of  $\text{Ti}_3\text{C}_2\text{T}_x\text{-BPS}$  in *m*-xylene and, b) specific capacitance of  $\text{Ti}_3\text{C}_2\text{T}_x$  (black curve) and  $\text{Ti}_3\text{C}_2\text{T}_x\text{-BPS}$  (red curve) at different scan rates. 1 M  $\text{H}_2\text{SO}_4$  was used as aqueous electrolyte, Pt wire as counter electrode and Ag/AgCl as reference electrode.

At UNISTRA, the electrochemical characterization in a three-electrode configuration with 1 M  $\text{H}_2\text{SO}_4$  electrolyte demonstrated that the  $\text{Ti}_3\text{C}_2\text{T}_x\text{-BPS}$  sample prepared in *m*-xylene exhibited the best performance, with a specific capacitance of 490 F/g at 10 mV/s, see Figure 17. In full cell,  $\text{Ti}_3\text{C}_2\text{T}_x\text{-BPS//AC}$  has shown excellent rate capability and long-term cycling stability, retaining 88.36% of its initial capacitance after 15000 cycles. In contrast, the pristine sample suffered faster degradation due to structural instability. These results confirm that UNISTRA water-based slurry formulation using  $\text{Ti}_3\text{C}_2\text{T}_x\text{-BPS}$  prepared in *m*-xylene meets the key performance targets for WP3: high conductivity, strong capacitance, low  $R_s$ , and excellent cycling durability in aqueous conditions.

### 3.7 BeDimensional MXene-based slurries

The CV plots shown in Figure 18 demonstrate the pseudocapacitive nature of the MXene-based electrodes across all electrolytes. Characteristic redox peaks, visible even at high scan rates, indicate Faradaic charge storage mechanisms associated with surface redox reactions and ion intercalation. In 3 M  $\text{H}_2\text{SO}_4$ , distinct and strong redox peaks are observed, consistent with reversible redox reactions involving  $\text{H}^+$  ions. The small size and high mobility of  $\text{H}^+$  ions facilitate deep intercalation and rapid kinetics, resulting in high current response.

In 8 m  $\text{NaNO}_3$ , moderate redox features are detected.  $\text{Na}^+$  ions, being larger and less mobile than protons, result in slower diffusion and weaker interactions with the MXene surface.

In 1 M KOH, the redox activity is slightly more pronounced than  $\text{NaNO}_3$ , likely due to the smaller hydrated radius and higher ionic conductivity of  $\text{K}^+$  compared to  $\text{Na}^+$ . The CV curve deformation at higher scan rates is more noticeable in neutral and basic media, implying that these systems are more diffusion-limited under fast charging conditions.

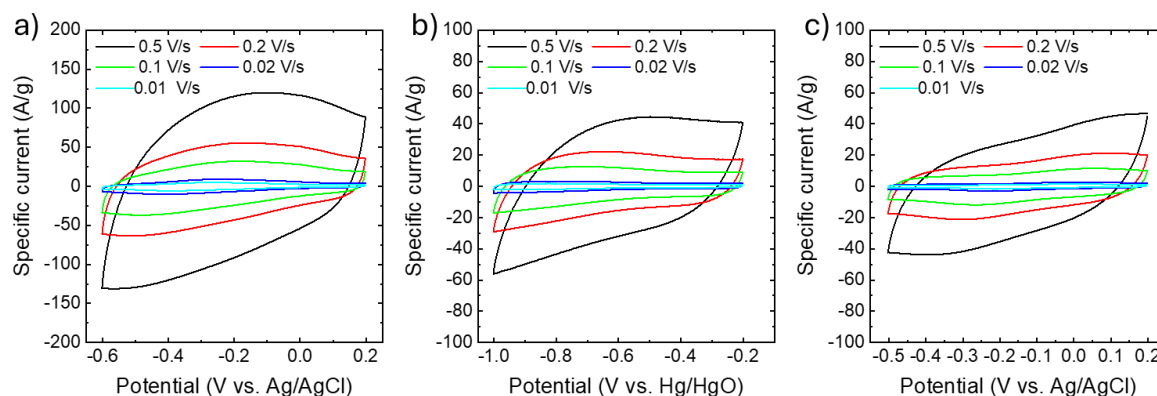


*Figure 18. Cyclic voltammetry of MXene-based electrodes in the presence of a) 3M H<sub>2</sub>SO<sub>4</sub>, b) 8 m NaNO<sub>3</sub>, and c) 1M KOH in different scan rate ranging from 10 to 500 mV s<sup>-1</sup>.*

Furthermore, GCD profiles confirm the pseudocapacitive behavior of the electrodes. As shown in Figure 19, the specific capacitance values obtained at 1 A g<sup>-1</sup> were 298 F g<sup>-1</sup> in 3 M H<sub>2</sub>SO<sub>4</sub>, 101 F g<sup>-1</sup> in 8 m NaNO<sub>3</sub>, and 134 F g<sup>-1</sup> in 1 M KOH. These values are consistent with the ion-accessibility trends observed in the CV curves. The superior performance in acidic electrolytes is attributed to facile H<sup>+</sup> intercalation and rapid redox activity. The lower capacitance in neutral and basic electrolytes reflects more limited ion transport and weaker electrochemical interaction. Capacitance retention at 20 A g<sup>-1</sup> was 76% in 3 M H<sub>2</sub>SO<sub>4</sub>, 73% in 8 m NaNO<sub>3</sub>, 63% in 1 M KOH. These retention values indicate excellent rate capability, especially in acidic and neutral conditions, even at high current densities. The combination of FLG and MXene contributes to this behavior. FLG acts as a conductive framework that enhances the overall electrical conductivity of the composite, prevents MXene restacking, maintaining accessible surface area, and facilitates electrolyte penetration and ion transport pathways. Together, these effects result in improved electrochemical kinetics and more robust structural stability under fast cycling conditions.

The successful implementation of a slurry-based, blade-compatible electrode preparation method demonstrates the scalability of MXene-FLG-PVDF composites. Compared to traditional vacuum filtration, this approach supports industrial electrode manufacturing while maintaining excellent electrochemical performance. In fact, the capacitance values achieved here surpass those of freestanding MXene electrodes reported previously, especially in acidic media.

These findings provide a robust baseline for subsequent evaluation of these electrodes in more complex systems, including protic ILs under development by SOLV in WP1.

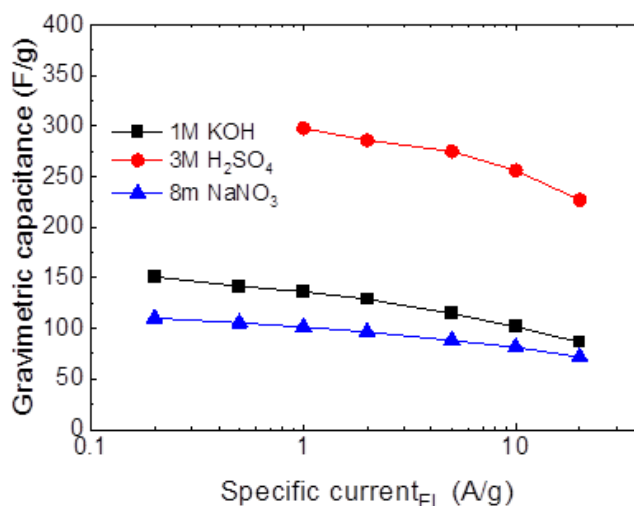


Figure 19. Gravimetric capacitances as a function of the specific current measured for MXene-based electrodes produced by slurry method.

At BED, the  $R_s$  of MXene-based free-standing electrodes provided by CU was measured using a four-probe conductivity method. The  $R_s$  ranged from  $300 \text{ m}\Omega/\square$  to  $1 \text{ }\Omega/\square$  as shown in Figure 20, well below the project target of  $<100 \text{ }\Omega/\square$  for each electrode composition.

To enhance the overall electrochemical performance even further, especially the capacitance retention and rate capability, the optimization of the mass ratio of FLG to MXene is currently under investigation. While MXenes possess outstanding intrinsic conductivity and pseudocapacitive behavior by themselves, they are prone to restacking as a consequence of strong interplane forces, hindering the access to the electrolyte and the efficiency of ion diffusion. FLG incorporation has several synergistic roles: as an electrically conductive spacer to prevent restacking and an enhancement of the electrical conductivity within the electrode that allows superior ion transport.

Additionally, FLG enhances the mechanical stability of the free-standing films, helping to prevent cracking or delamination during cycling. It also improves slurry processability and coating uniformity, which are essential for scale-up. Importantly, the hybrid structure offers a combination of fast EDLC response from FLG and pseudocapacitive contributions from MXenes, potentially leading to a more balanced trade-off between energy and power density. Furthermore, FLG may provide a degree of oxidative stabilization to MXene flakes under electrochemical operating conditions.

Together, these effects justify the strategic integration of FLG into MXene-based electrodes as an approach to utilize their full performance potential for high-power, durable, and scalable SC systems.

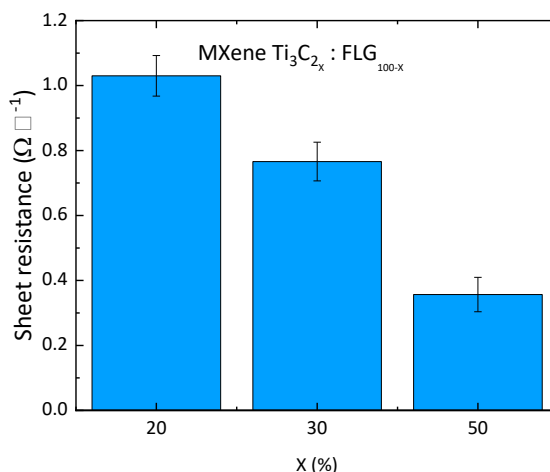


Figure 20. Sheet resistance of free-standing MXene-FLG electrodes.

### 3.8 Contribution to project (linked) Objectives

- Rs lower than 100 Ω/□, as low as 220 mΩ/□ for the CG:FLG:CMC-SBR slurry coated on carbon-coated aluminum collectors and 400 mΩ/□ for MXenes free-standing films..
- Maximization of the active material content (CG), up to 94 w%, and, therefore, of the gravimetric capacity and of the specific energy, whilst maintaining a Rs lower than 100 Ω/□.
- Implementation of sustainable fluorine-free water-based binder (CMC-based), minimizing the footprint of the electrodes and of their production processes.
- Implementation of IG-based slurry. It simplifies the cell production process by eliminating the pre-filling step and improves the rate performances thanks to the higher electrolyte permeation in the electrodes.
- Easy processability through printing deposition techniques, including doctor blading.

### 3.9 Contribution to major project exploitable result

- Development of novel electrode slurries based on 2D materials

## 4 Conclusion and Recommendation

In conclusion, within Task 3.1, graphene-based slurry formulations were developed and evaluated by TUD, UCAM, and BED. Specifically, TUD developed a polyaniline-functionalized electrochemically EG-based slurry, focusing on its processability and performance in aqueous electrolytes. UCAM optimized slurries based on HPH-FLG, establishing a correlation between specific surface area and  $R_s$ . BED investigated slurries based on CG, FLG, and a CMC binder mixed with SBR. Specifically, CG demonstrated a significantly lower  $R_s$  ( $37 \Omega/\square$ ) compared to AC ( $352 \Omega/\square$ ), which was further reduced to  $29 \Omega/\square$  through the incorporation of FLG. These values meet the GREENCAP project target of  $R_s < 100 \Omega/\square$ .

Importantly, the state-of-the-art PVDF binder was successfully replaced with fluorine-free CMC, enabling the use of water as a solvent in place of NMP. This substitution simplifies the manufacturing process and eliminates safety and environmental concerns associated with NMP, including the need for high temperature drying and hazardous handling procedures.

The conductivity values obtained for the pristine materials were validated using four-probe conductivity measurements on slurries deposited on carbon-coated aluminum collectors. A conductivity of  $5.6 \times 10^4 \text{ S/cm}$  was achieved, corresponding to a sheet resistance of  $220 \text{ m}\Omega/\square$  for electrodes with a thickness of  $70 \mu\text{m}$  and a mass loading of  $5.2 \text{ mg/cm}^2$ .

In parallel SKL developed CDC-based slurries with minimal binder content, successfully maximizing the active material loading while maintaining processability.

Furthermore, MXene-based slurries, provided by TCD and CU, were investigated by UNISTRA and BED. These included free-standing films, FLG-hybridized composites, and binder-assisted formulations compatible with conventional coating processes. All demonstrated promising performance in terms of both specific capacitance and electrical conductivity.

Finally, an IG-based slurry approach was explored, showing improved electrode wetting and significantly enhanced rate capability, supporting its potential for high-power SC applications.

## 5 Risks and interconnections

### 5.1 Risks/problems encountered

No major risks encountered during this task

### 5.2 Interconnections with other deliverables

The Task 3.1, described in the current document, exploited the results of WP1 and WP2 for developing the electrode slurries. Moreover, its results are exploited in Task 3.2, which is dedicated to the validation of the electrodes in pouch cell prototypes and in the deliverables 4.1 and 4.3 which describes the efforts for the upscaling of the materials, of the slurries and to the development of a industrial prototype, i.e. a cylindrical cell.

## 6 References

## 7 Acknowledgement

The author(s) would like to thank the partners in the project for their valuable comments on previous drafts and for performing the review.

### Project partners:

#	Partner short name	Partner Full Name
1	BED	BEDIMENSIONAL SPA
2	SOLV	SOLVIONIC
3	FSU	FRIEDRICH-SCHILLER-UNIVERSITÄT JENA
4	SKL	SKELETON TECHNOLOGIES OU
5	TCD	THE PROVOST, FELLOWS, FOUNDATION SCHOLARS & THE OTHER MEMBERS OF BOARD, OF THE COLLEGE OF THE HOLY & UNDIVIDED TRINITY OF QUEEN ELIZABETH NEAR DUBLIN
6	TUD	TECHNISCHE UNIVERSITÄT DRESDEN
7	UNISTRA	UNIVERSITÉ DE STRASBOURG
8	SM	SKELETON MATERIALS GMBH
9	UNR	UNIRESEARCH BV
10	CNR	CONSIGLIO NAZIONALE DELLE RICERCHE
11	UCAM	THE CHANCELLOR MASTERS AND SCHOLARS OF THE UNIVERSITY OF CAMBRIDGE
12	CU	Y CARBON LLC

### Disclaimer/ Acknowledgment



Copyright ©, all rights reserved. This document or any part thereof may not be made public or disclosed, copied or otherwise reproduced or used in any form or by any means, without prior permission in writing from the GREENCAP Consortium. Neither the GREENCAP Consortium nor any of its members, their officers, employees or agents shall be liable or responsible, in negligence or otherwise, for any loss, damage or expense whatever sustained by any person as a result of the use, in any manner or form, of any knowledge, information or data contained in this document, or due to any inaccuracy, omission or error therein contained.

All Intellectual Property Rights, know-how and information provided by and/or arising from this document, such as designs, documentation, as well as preparatory material in that regard, is and shall remain the exclusive property of the GREENCAP Consortium and any of its members or its licensors. Nothing contained in this document shall give, or shall be construed as giving, any right, title, ownership, interest, license or any other right in or to any IP, know-how and information.

This project has received funding from the European Union's Horizon Europe research and innovation programme under grant agreement No 101091572. Views and opinions expressed are however those of the author(s) only and do not necessarily reflect those of the European Union. Neither the European Union nor the granting authority can be held responsible for them.